HHS Public Access

Author manuscript

Cancer Res. Author manuscript; available in PMC 2018 February 15.

Published in final edited form as:

Cancer Res. 2017 February 15; 77(4): 874–885. doi:10.1158/0008-5472.CAN-16-2170.

ESE3 inhibits pancreatic cancer metastasis by upregulating E-cadherin

Tiansuo Zhao[1,2], **Wenna Jiang**[1], **Xiuchao Wang**[1], **Hongwei Wang**[1], **Chen Zheng**[1], **Yang Li**[1], **Yan Sun**[3], **Chongbiao Huang**[1], **Zhi-bo Han**[4], **Shengyu Yang**[5], **Zhiliang Jia**[2], **Keping Xie**[2], **He Ren**[1], and **Jihui Hao**[1]

[1]Tianjin Medical University Cancer Institute and Hospital, National Clinical Research Center for Cancer; Key Laboratory of Cancer Prevention and Therapy, Department of Pancreatic Cancer, Tianjin, PR China.

[2]Department of Gastroenterology, Hepatology and Nutrition, The University of Texas MD Anderson Cancer Center, Houston, Texas.

[3]Department of Pathology, Tianjin Medical University Cancer Institute and Hospital, Tianjin, PR China.

[4]Institute of Hematology and Hospital of Blood Diseases, Chinese Academy of Medical Sciences and Peking Union Medical College, Tianjin, PR China.

[5]Department of Tumor Biology and Comprehensive Melanoma Research Center, H. Lee Moffitt Cancer Center and Research Institute, Tampa, Florida.

Abstract

The ETS family transcription factor ESE3 is a crucial element in differentiation and development programs for many epithelial tissues. Here we report its role as a tumor suppressor in pancreatic cancer. We observed drastically lower ESE3 expression in pancreatic ductal adenocarcinomas (PDAC) compared to adjacent normal pancreatic tissue. Reduced expression of ESE3 in PDAC correlated closely with an increase in lymph node metastasis and vessel invasion and a decrease in relapse-free and overall survival in patients. In functional experiments, downregulating the expression of ESE3 promoted PDAC cell motility and invasiveness along with metastasis in an orthotopic mouse model. Mechanistic studies in PDAC cell lines, the orthotopic mouse model and human PDAC specimens demonstrated that ESE3 inhibited PDAC metastasis by directly upregulating E-cadherin expression at the level of its transcription. Collectively, our results establish ESE3 as a negative regulator of PDAC progression and metastasis by enforcing E-cadherin upregulation.

Corresponding Authors: Keping Xie, Department of Gastroenterology, Hepatology and Nutrition, Unit 1466, The University of Texas MD Anderson Cancer Center, 1515 Holcombe Boulevard, Houston, TX 77030. Phone: 713-794-5073; Fax: 713-745-3654; kepxie@mdanderson.org; or He Ren, Department of Pancreatic Cancer, Tianjin Medical University Cancer Institute and Hospital, Tianjin 300060, PR China. Phone: 86-022-23340123; renhe@tjmuch.com.
The first two authors contributed equally to this work.

Disclosure of Potential Conflicts of Interest
No potential conflicts of interest were disclosed.

Keywords

Pancreatic ductal adenocarcinoma; ESE3; E-cadherin; Metastasis

Introduction

Pancreatic ductal adenocarcinoma (PDAC) is the leading cause of cancer-related deaths in the United States, with a dismal 5-year survival rate of no more than 6% (1). Despite recent improvements in PDAC diagnosis and therapy, most pancreatic cancer patients die of invasion and metastasis to the regional lymph nodes and/or distant organs (2,3). Unfortunately, the underlying mechanism for PDAC invasion and metastasis remain poorly understood. Therefore, improved understanding of the molecular mechanisms underlying pancreatic cancer invasion and metastasis is an urgent need for designing effective interventional strategies and prolonging patient life (3,4).

The ETS gene family consists of nearly 40 distinct members (5). Each ETS transcription factor possesses a highly conserved DNA-binding domain and binds to a conserved ETS-binding site (EBS; GGAA/T) in the promoter/enhancer regions of target genes (6,7). Increasing evidence implicates roles for these transcription factors in tissue differentiation (8) and tumor progression (9–11). A subset of ETS factors known as epithelium-specific ETS (ESE) factors, including ESE1 (Ert/Jen/Elf3/Esx), ESE2 (Elf5), ESE3 (EHF), and Pdef (Pse), are expressed in epithelial tissues (12). Authors reported that ESE3 in particular binds directly to target genes to control epithelial-to-mesenchymal transition (EMT), stem-like features (13,14), and tumor progression (15–17). Feldman and coworkers have analyzed the expression patterns of ESE factors in diverse types of tissues and cell lines, and found that in normal human pancreas only ESE1 and ESE3 but not ESE2 and Pdef proteins are expressed (5). However, the role of ESE3 in PDAC development and progression has yet to be examined.

The classical cadherins are cell surface glycoproteins that mediate calcium-dependent cell-cell adhesion primarily in a homophilic manner (18–21). Their adhesion-regulating function requires interaction with the actin cytoskeleton via catenins. Cadherins are known to play important roles in tumor development and progression (19,22). In late-stage tumorigenesis, switching of the cadherin subtype from E-cadherin to N-cadherin occurs during tumor-cell invasion and metastasis and is mechanistically associated with EMT (23,24). Cadherin switching usually refers to a change in expression from E-cadherin to N-cadherin (25–28). Interestingly, changes in E-cadherin expression in the pancreas may play a role in human pancreatic intraepithelial neoplasia development (29). Specifically, researchers found that E-cadherin expression was lower at the membrane but higher in the cytoplasm in pancreatic intraepithelial neoplasia cells than in normal ductal cells (29). The roles of E-cadherin in pancreatic cancer development and progression are well documented (30–34). However, the molecular mechanisms underlying altered E-cadherin expression in pancreatic cancer cells remain unclear.

In the present study, we explored the functions of ESE3 in PDAC invasion and metastasis. Our data demonstrated that ESE3 expression was reduced in PDAC cell lines and human

PDAC specimens. Also, ESE3 downregulation promoted PDAC cell migration and invasion *in vitro* and metastasis in orthotopic mouse models. Importantly, ESE3 mechanistically suppressed PDAC metastasis by upregulating E-cadherin protein expression in PDAC cells via direct binding to the promoter of the E-cadherin gene.

Materials and Methods

Cell culture and regents

The human PDAC cell lines AsPC-1, CFPAC-1, BxPC-3, PANC-1 and MIA-PaCa-2 were obtained from the Committee of Type Culture Collection of Chinese Academy of Sciences or were purchased from the American Type Culture Collection (Manassas, VA). All of the cell lines were obtained in 2013 and authenticated in August 2015 using short tandem repeat analysis. These cells grew at 37°C in a humidified atmosphere of 95% air and 5% CO_2 using Dulbecco's modified Eagle's medium with 10% fetal bovine serum. 5-aza-2'-deoxycytidine (5-AdC) and MS-275 were purchased from Sigma-Aldrich.

Western blot analysis

Western blot analysis of protein expression was performed as described previously (3). Briefly, protein lysates (20 μg) were separated using sodium dodecyl sulfate-polyacrylamide gel electrophoresis, and target proteins were detected using Western blotting with antibodies against ESE3 (1:1000), E-cadherin (1:1000), and β-actin (1:1000) (details are summarized in supplementary Table S1).

Reverse transcription-polymerase chain reaction

Total RNA was extracted from treated PDAC cells using TRIzol reagent (Invitrogen) and used in first-strand cDNA synthesis with a First-Strand Synthesis System for reverse transcription-polymerase chain reaction (RT-PCR; Takara). Each RT-PCR experiment was performed independently at least three times. The PCR primers used are listed in supplementary Table S1.

MTT and Colony Formation Assays

To determine the viability of PANC-1 and MIA-PaCa-2 cells after treatment of 5-AdC, MTT assay was used (35,36). In brief, the cells were seeded at a concentration of 1×10^4 cells per well in 96-well plates. Twenty-four hours after seeding, the attached cells were treated with different concentrations of 5-AdC. After 48-hour incubation with 5-AdC, the medium was removed and replaced with 100 μL per well of fresh medium containing 20 μL of MTT reagent (5 mg/mL) and incubated for 4 hours at 37°C. Then 100 μL of dimethyl sulfoxide was added, and the optical density was measured at 550 nm using an ELISA plate reader. For colony formation assay, PANC-1 and MIA-PaCa-2 cells were seeded in 6-well plates with 100 cells per well. After incubation with 14 days, colonies were stained with crystal violet and counted (37,38).

Immunofluorescence

To evaluate the expression and distribution of E-cadherin in PDACs after regulated ESE3 expression, PDAC cells were seeded onto glass slides, washed with phosphate-buffered saline, fixed with 4% paraformaldehyde for 15 minutes, permeabilized with 0.1% Triton X-100 in phosphate-buffered saline for 15 minutes at room temperature, and blocked for 1 hour with 3% bovine serum albumin in phosphate-buffered saline. The cells were then stained with an anti-E-cadherin antibody (1:200 dilution) overnight at 4°C. Cells were mounted with 4’,6-diamidino-2-phenylindole (DAPI) Fluoromount-G medium and a DAPI nuclear stain (SouthernBiotech). The slides were viewed under an Olympus microscope.

Chromatin immunoprecipitation assay

A chromatin immunoprecipitation assay was performed using a commercially available kit (Upstate Biotechnology) according to the manufacturer’s instructions (3,34). PCR analysis was performed using primer sets spanning four regions comprising the EBSs identified in the human E-cadherin promoter. PCR products were analyzed using gel electrophoresis. The primer sequences are listed in supplementary Table S1.

Gene expression alteration and determination

Small interfering RNAs (siRNAs) against ESE3 were designed and synthesized from GenePharma (supplementary Table S1). Also, human ESE3 cDNA was cloned into a pCDH plasmid expression vector (pCDH-ESE3). Lentiviral infections were performed according to standard procedures. Briefly, HEK293 cells were co-transfected with the plasmids pMD2.G and psPAX2 (Addgene) along with either pCDH-ESE3 or pCDH-Vector using the jetPRIME transfection reagent (Polyplus-transfection) according to the manufacturer’s protocol. Twelve hours later, the transfection medium was replaced with fresh Dulbecco’s modified Eagle’s medium with 10% fetal bovine serum. Forty-eight hours afterward, the viral supernatants were collected and concentrated using Centricon Plus-70 filter units (EMD Millipore). In addition, PANC-1 cells were infected overnight with viral supernatants supplemented with 8 μg/mL hexadimethrine bromide (Polybrene; Sigma). Two days after infection, stably transduced PANC-1 cells were selected with 1 μg/mL puromycin for 7 days, resulting in a homogeneous population of 100% puromycin-resistant cells.

Genomic DNA fragments of the human E-cadherin gene spanning +1 to −1193 bp (GenBank accession number: L34545.1) relative to the transcription initiation sites were generated using PCR and inserted into pGL3-Basic vectors (denoted as pGL3-E-cadherin). All constructs were sequenced to confirm their identities. A Dual-Luciferase Reporter Assay System (Promega) was used to measure the luciferase activity in transfected cells as described previously (3,39).

PDAC cell lines were seeded in six-well plates at a density of 5×10^5 cells/well for transfection. When the cells were 80% confluent, siRNA duplexes or plasmids were transfected into them using Lipofectamine 2000 (Invitrogen) for 48 hours. The cells were harvested for testing including cell migration and invasion, Western blot, reverse transcription-PCR, and immunofluorescent analysis.

Wound-healing and cell migration assays

A wound-healing assay and migration assays were performed using indicated cells according to a published protocol (3,40). The invasion assay was performed using filters coated with one-sixth diluted Matrigel (BD Bioscience). Dulbecco's modified Eagle's medium with 10% fetal bovine serum was added to the lower chamber of Boyden chamber, and cells treated as indicated were allowed to incubate for 36 hours. Cells that migrated to the bottoms of the filters were stained using a three-step stain set (Thermo Fisher Scientific).

Animals and orthotopic and intrasplenic mouse models of pancreatic cancer metastasis

All animal studies were conducted under an approved protocol by Tianjin Cancer Institute and Hospital and MD Anderson Cancer Center in accordance with the principles and procedures outlined in the National Institutes of Health Guide for the Care and Use of Laboratory Animals. For orthotopic pancreatic tumor cell injection, nude nu/nu mice were placed in two groups (PANC-1/pCDH-Vector and PANC-1/pCDH-ESE3, six mice per group). PANC-1 cells (2×10^6) were injected into the pancreases of the mice. In each mouse, the pancreas was then returned to the peritoneal cavity, and the skin incision was closed with skin clips. Then, nude nu/nu mice were given intrasplenic injections of stable PANC-1/pCDH-Vector or PANC-1/pCDH-ESE3 cells (41). Eight weeks later, the visible metastatic lesions in the gut, mesentery, and liver of each mouse were counted (42).

Patient specimens and immunohistochemistry

With approval from the Ethics Committee at the Tianjin Cancer Institute and Hospital, tissue microarrays (TMAs) containing PDAC and adjacent normal pancreatic tissue specimens were obtained from patients who underwent surgical resection after histopathologic diagnosis of PDAC at that institution. The patients' histopathologic and clinical characteristics are shown in Table S2. Immunohistochemical analysis of the TMA specimens for ESE3 and E-cadherin expression was performed using a DAB substrate kit (Maxin). Immunoreactivity was semiquantitatively scored according to the estimated percentage of tumor cells positive ESE3 expression as described previously (3). The staining intensity for the specimens was scored as 0 (negative), 1 (low), 2 (medium), or 3 (high). Also, the staining extent was scored as 0 (0% stained), 1 (1–25% stained), 2 (26–50% stained), and 3 (51–100% stained). The final staining scores were determined by multiplying the intensity scores by the staining extent and ranged from 0 to 9. Final scores (intensity score × percentage score) lower than 2 were considered to represent negative staining (−), scores of 2 or 3 were considered to represent low staining (+), scores of 4 to 6 were considered to represent moderate staining (++), and scores higher than 6 were considered to represent high staining (+++).

Statistical analysis

The Student *t*-test for paired data was used to compare mean values. Analysis of variance was used to examine two groups' data with continuous variables. Categorical data were analyzed using either the Fisher exact or χ^2 test. Each experiment was conducted independently at least three times, and values were presented as the means ± standard error of the mean (SEM) unless otherwise stated. The statistical analyses were performed using

the SPSS software program (version 21.0; IBM Corporation). Statistical significance was indicated by a conventional *P* value less than 0.05.

Results

ESE3 expression is reduced in PDAC specimens

We first examined the expression of ESE3 in a TMA consisting of human PDAC and adjacent normal pancreatic tissue specimens. The expression of ESE3 was significantly lower in the PDACs than in the normal tissue ($P < 0.001$) (Fig. 1A). We then analyzed the ESE3 expression in the TMA specimens according to staining score and found lower ESE3 expression in ductal cells in tumor specimens than in normal ductal cells ($P < 0.001$) (Fig. 1B). To determine the role of ESE3 in PDAC progression, we evaluated the correlation between ESE3 expression and histologic PDAC grade. Interestingly, nuclear ESE3 expression levels were inversely correlated with the histological grade of PDAC (Fig. 1A; Table 1). We further investigated ESE3 expression in PDAC and paired adjacent normal pancreatic tissue specimens. Despite some interindividual variations, ESE3 protein expression was remarkably lower in PDACs than in normal tissue ($P < 0.05$) (Fig. 1C), suggesting that ESE3 expression decreased in the PDACs during progression. Intriguingly, in pancreatic neoplasms other than PDAC, such as serous cystadenomas, neuroendocrine tumors, and intraductal papillary mucinous neoplasms, ESE3 expression remained high (Fig. 1D).

Authors reported that ESE3 protein expression can be silenced by methylation at an evolutionarily conserved CpG site in its promoter in prostate cancer cells and can be restored by treatment with the DNA methylation inhibitor 5-AdC (15). Thus, we treated MIA-PaCa-2 PDAC cells with MS-275 (a synthetic histone deacetylase inhibitor) and 5-AdC. The results demonstrated that ESE3 mRNA and protein expression increased after treatment with both agents (Fig. 1E). Taken together, these data demonstrated that downregulation of ESE3 expression may be an early and universal event during PDAC progression and result from methylation of the ESE3 promoter.

Loss of ESE3 expression in PDACs is associated with poor overall and relapse-free survival

To determine the pathologic significance of ESE3 expression regarding PDAC progression, we evaluated the correlation between ESE3 expression and established PDAC prognostic factors (Table 1). We did not find an obvious correlation of expression of ESE3 with age, sex, or tumor size in PDAC patients. However, ESE3 expression was negatively correlated with histologic grade ($\chi^2 = 7.275$, $P < 0.05$, $r = -0.260$), lymph node metastasis ($\chi^2 = 6.358$, $P < 0.05$, $r = -0.243$), and vessel invasion ($\chi^2 = 8.058$, $P < 0.01$, $r = -0.273$) in PDAC specimens (Table 1). Importantly, Kaplan-Meier analysis of TMA data according to ESE3 expression indicated that PDAC patients with negative (−) or low (+) ESE3 protein expression had significantly worse median overall survival (OS) and relapse-free survival (RFS) durations than did those with moderate (++) or high (+++) ESE3 protein expression ($P < 0.001$; OS: 9 and 20 months, respectively; RFS: 4 and 12 months, respectively) (Fig. 1F and 1G). We have further analyzed the clinical data and found that metastasis (81.25%) was

the main reason for a shorter RFS in the low-ESE3 group. To explore the role of ESE3 in PDAC progression, we performed univariate and multivariate analyses of clinical follow-up data for our cohort of PDAC patients (Table 2). Consistently, ESE3 expression was positively correlated with both OS and RFS in both analyses, *i.e.*, loss of ESE3 expression predicted shorter OS and RFS, supporting that loss of ESE3 expression is an independent risk factor for PDAC progression.

5-AdC inhibited proliferation, migration and invasion of PDAC cells and increased expression of ESE3 suppressed the proliferation of PDAC cells

To explore the effect of 5-AdC on cellular viability, migration and invasion of PDAC cells, we treated of PANC-1 and MIA-PaCa-2 PDAC cells with different concentrations of 5-AdC. MTT, colony-formation, wound healing and transwell migration and invasion assays were performed. We found that the viability and colony-forming ability of PANC-1 and MIA-PaCa-2 PDAC cells were inhibited by 5-AdC (supplementary Fig. S1A and S1B, $P < 0.01$). 5-AdC also suppressed the migration and invasion of PANC-1 and MIA-PaCa-2 cells (supplementary Fig. S1C and S1D, $P < 0.01$) (22,23). Also, we observed that ESE3 suppressed anchorage-dependent colony-forming activities of PANC-1 and MIA-PaCa-2 cells ($P < 0.05$) (supplementary Fig. S1E). Importantly, expression of cleaved poly (ADP-ribose) polymerase (PARP) protein was upregulated in PANC-1 cells transfected with pCDH-ESE3 and downregulated in MIA-PaCa-2 cells transfected with ESE3 siRNA (siESE3; $P < 0.01$) (supplementary Fig. S1F). These data suggested that 5-AdC can inhibit proliferation, migration and invasion of PDAC cells. An increased expression of ESE3 suppressed proliferation of PDAC cells, whereas decreased expression of ESE3 did the opposite.

ESE3 inhibits PDAC cell proliferation, migration, and invasion

To determine whether ESE3 overexpression alone is sufficient to suppress PDAC cell migration, we induced ectopic expression of ESE3 in two PDAC cell lines with low endogenous ESE3 expression (PANC-1 and AsPC-1) (supplementary Fig. S2). We examined the resulting cell migration and invasion using a Transwell assay. We found that ESE3 upregulation reduced PANC-1 and AsPC-1 cell migration and invasion ($P < 0.05$) (Fig. 2A and 2B). Wound-healing assays demonstrated that ESE3 overexpression inhibited the migratory activity of both PDAC cell lines more so than that of control cells (Fig. 2C).

To determine the role of ESE3 in the suppressive phenotypes of PDAC cells *in vitro*, we transfected two PDAC cell lines with high endogenous ESE3 expression (CFPAC-1 and BxPC-3) with three pairs of siRNAs (siRNA #1, #2, and #3) to knock down their ESE3 expression (Fig. 3C). Of these three pairs of siRNAs, siRNA #3 most efficiently knocked down ESE3 expression, doing so by more than 70%; we therefore used it in subsequent functional studies. Cell migration and invasion analysis using a Transwell assay suggested that ESE3 depletion in CFPAC-1 and BxPC-3 cells increased cell migration and invasion (Fig. 2D and 2E). In wound-healing assays, ESE3 silencing also increased the migratory activity of CFPAC-1 and BxPC-3 cells (Fig. 2F). These data indicated that loss of ESE3 expression in PDAC cells is critical for their growth, migration, and invasion.

ESE3 expression is positively correlated with E-cadherin expression in PDAC cell lines

As described above, ESE3 expression was downregulated in progression of PDAC and inhibited the migration and invasion of PDAC cell lines. To identify the mechanism of migration of PDACs, we transfected PANC-1 and CFPAC-1 cells with pCDH-ESE3 and siESE3 and evaluated the expression of EMT markers (E-cadherin, Snail and Vimentin) in them using Western blotting (Fig. 3; supplementary Fig. S3). Of these EMT-related proteins, E-cadherin was the most upregulated and downregulated in PANC-1 and CFPAC-1 cells, respectively, after ESE3 overexpression and knockdown. To verify the positive relationship between ESE3 and E-cadherin expression, we performed Western blotting, reverse transcription-PCR, and immunofluorescent analysis to assess the changes in E-cadherin expression in PDAC cell lines after ESE3 overexpression. We observed that expression of E-cadherin protein and mRNA was upegulated and that ESE3 was overexpressed in PANC-1 (Fig. 3A) and AsPC-1 (Fig. 3B) cells. Conversely, expression of E-cadherin protein and mRNA was downregulated in CFPAC-1 (Fig. 3C) and BxPC-3 (Fig. 3D) cells after knockdown of expression of ESE3 with siRNA (Fig. 3C and 3D, bottom panel).

ESE3 overexpression inhibits PDAC metastasis by regulating E-cadherin expression

To further understand the role of ESE3 in E-cadherin–mediated PDAC migration, we induced ectopic ESE3 expression in CFPAC-1 and BxPC-3 cells with knockdown of E-cadherin expression (Fig. 3E and 3F). As shown in Fig. 3G and 3H, knockdown of E-cadherin overexpression enhanced the migration of PDAC cells. However, ESE3 overexpression at least partially inhibited the effect of E-cadherin knockdown on PDAC cell migration ($P < 0.05$), suggesting that E-cadherin was involved in ESE3-mediated cell migration.

Ectopic ESE3 expression suppresses PDAC metastasis in orthotopic and intrasplenic PDAC models

To determine whether ESE3 suppresses PDAC metastasis, we investigated the effects of ectopically overexpressed ESE3 on PDAC metastasis in orthotopic and intrasplenic mouse models. After orthotopic or intrasplenic injection in mice, control PANC-1/pCDH-Vector cells generated primary tumors in the pancreas and distant metastases in the liver, gut, and mesentery over 8 weeks. Also, in mice injected with PANC-1/pCDH-ESE3 cells, the sizes of the primary pancreatic tumors and metastases in the liver, gut, and mesentery decreased dramatically after induction of ectopic ESE3 expression (mean ± SEM, 28.17 ± 9.15 versus 4.00 ± 1.79; $P < 0.001$) (Fig. 4A and 4B; supplementary Fig. S4). To evaluate the association between ESE3 and E-cadherin expression in PDACs, we performed Western blot (Fig. 4C) and immunohistochemical (Fig. 4D) analysis of orthotopic pancreatic tumors in nude mice injected with PANC-1/pCDH-Vector and stable PANC-1/pCDH-ESE3 cells. The results suggested that expression of E-cadherin increased with overexpression of ESE3 *in vivo*. Collectively, these data demonstrated that ESE3 suppressed the proliferation and metastasis of orthotopic and intrasplenic PDACs and confirmed the positive association between ESE3 and E-cadherin expression in PDACs *in vivo*. Taken together, our data indicated that ESE3 is a critical suppressor of PDAC metastasis in mouse models.

ESE3 expression positively correlates with E-cadherin expression in human PDACs

To determine whether ESE3 indeed regulates the expression of E-cadherin in PDAC patients, we performed immunohistochemical staining of human PDAC specimens to measure the ESE3 and E-cadherin expression in them. As shown in Figure 4E, E-cadherin expression co-localized with ESE3 expression in consecutive sections of PDACs with high and low differentiation grades. Importantly, ESE3 expression in PDAC specimens was highly positively correlated with E-cadherin expression (Fig. 4F and 4G), implicating ESE3 as a critical regulator of E-cadherin expression in PDAC patients. To further determine whether this finding is clinically relevant, we investigated the expression of ESE3 and E-cadherin in 179 PDACs with RNA sequencing data available from The Cancer Genome Atlas ($P < 0.001$) (Fig. 4H) (43,44). Importantly, Kaplan-Meier analysis of TMA data according to ESE3 and E-cadherin expression revealed that patients with negative expression for both E-cadherin and ESE3 had significant shorter survival duration (OS: 9 months; RFS: 4 months), while patients with positive expression for both E-cadherin and ESE3 had significant longer survival duration (OS: 20 months; RFS: 12 months). Patients with negative expression for either E-cadherin or ESE3 had survival duration (OS: 12 months; RFS: 5 months) between the other two groups. The differences in patient survival among those three groups were highly significant ($P<0.001$) (Fig. 4I and 4J). These results demonstrated that ESE3 expression was positively associated with E-cadherin expression in human PDAC specimens and ESE3 and E-cadherin protein expression impacted the OS and RFS of PDAC patients.

ESE3 directly regulates the expression of E-cadherin in PDACs by binding to the EBS in the E-cadherin gene promoter

To determine whether ESE3 directly regulates transcription of E-cadherin in pancreatic cancer cells, we examined the promoter region of the human E-cadherin gene and identified six EBSs in it (Fig. 5A). To see whether ESE3 binds directly to the E-cadherin promoter, we performed a chromatin immunoprecipitation assay using the PANC-1 cell line. In chromatin fractions pulled down by an anti-ESE3 antibody, we detected EBS1, EBS2, and EBS3 in the E-cadherin promoter (Fig. 5B). The fraction immunoprecipitated by the anti-ESE3 antibody increased significantly ($P < 0.01$) with ESE3 overexpression, suggesting that ESE3 expression influenced the binding of ESE3 to the E-cadherin promoter.

To determine whether binding of ESE3 to the E-cadherin promoter activates the promoter, we constructed three E-cadherin luciferase promoter vectors—pGL3-EBS(1), containing −302 to −1 bp; pGL3-EBS(2), containing −488 to −1; and pGL3-EBS (full-length), containing −1168 to −1 and transfected them with or without an ESE3 expression vector (pCDH-ESE3) into HEK293 and PANC-1 cells. Luciferase analysis demonstrated that ESE3 overexpression significantly increased E-cadherin promoter activity at different promoter vector lengths in HEK293 ($P < 0.05$) (Fig. 5C, left panel) and PANC-1 ($P < 0.05$) (Fig. 5C, right panel) cells. Taken together, these results suggested that ESE3 can not only directly bind to the E-cadherin promoter but also influence the activity of E-cadherin in PDACs.

Discussion

In this study, we investigated the function of ESE3 in PDAC invasion and metastasis. We found drastically lower ESE3 expression in PDACs than in adjacent normal pancreatic tissue. Importantly, reduced ESE3 expression in PDACs was closely associated with increased PDAC lymph node metastasis and vessel invasion but reduced RFS and OS durations. Furthermore, downregulation of ESE3 expression promoted PDAC cell motility and invasiveness *in vitro* and metastasis in an orthotopic mouse model of pancreatic cancer. ESE3 expression inhibited PDAC metastasis by upregulating E-cadherin expression as demonstrated in PDAC cell lines, the orthotopic mouse model, and human PDAC specimens. Mechanistically, ESE3 bound directly to and transactivated the E-cadherin promoter, upregulating E-cadherin expression in PDAC cells. Collectively, these data demonstrated that ESE3 negatively regulates PDAC progression and metastasis by upregulating E-cadherin expression.

Authors have reported loss of ESE3 expression in esophageal squamous cell carcinoma (17) and prostate tumor (13,15,16) cases. We found that ESE3 expression levels were lower in PDACs than in matched normal pancreatic tissue specimens. PDAC patients negative for or with low ESE3 protein expression had markedly worse OS and RFS durations than did those with high or moderate ESE3 expression. Importantly, loss of ESE3 expression was closely correlated with poor PDAC prognosis in both univariate and multivariate analyses, suggesting that ESE3 expression levels are independent predictors of OS and RFS of PDAC. Therefore, loss of ESE3 plays an important role in PDAC development and progression.

In the present study, we discovered strong evidence supporting ESE3 as a tumor suppressor gene. We transfected PDAC cell lines with ESE3 plasmids and siRNA to evaluate their migration and invasion after gain or loss of their function. Transwell and wound-healing assay results suggested that ESE3 upregulation in PANC-1 and AsPC-1 cells reduced their migration and invasion. In contrast, ESE3 downregulation in CFPAC-1 and BxPC-3 cells increased their migration and invasion. To confirm the role of ESE3 in pancreatic cancer cell invasion and metastasis *in vivo*, we developed orthotopic and intrasplenic pancreatic cancer mouse models using injection of PANC-1/pCDH-Vector and PANC-1/pcDH-ESE3 cells. The results of experiments using these models indicated that ESE3 overexpression suppressed PDAC metastasis. Consistently, the data from these experiments indicated that ESE3 is a critical suppressor of the migration and invasion of PDAC *in vitro* and *in vivo*.

E-cadherin–regulated cell-cell adhesion is decreased in PDACs, and this adhesion is thought to be a prerequisite for acquisition of invasive and metastasis properties (45). Most importantly, loss of membranous E-cadherin expression in pancreatic cancer cells is correlated with lymph node metastasis, high tumor grade, and advanced disease stage (46). In the present study, we identified the mechanism by which ESE3 controls PDAC metastasis and progression. We evaluated the expression of the EMT markers E-cadherin, β-catenin, Snail, and vimentin in PDAC cell lines using Western blotting after transfection with pCDH-ESE3 and siESE3. We found that E-cadherin protein expression was positively correlated with ESE3 expression, suggesting that ESE3 regulates PDAC metastasis by upregulating E-cadherin protein expression.

To further understand the role of ESE3 in E-cadherin–mediated migration and invasion of PDACs, we induced ectopic expression of ESE3 in E-cadherin–knockdown CFPAC-1 and BxPC-3 cells. ESE3 overexpression was sufficient to inhibit ESE3 overexpression alone inhibited PDAC migration and metastasis *in vitro* and *in vivo*. Furthermore, ESE3 expression was positively associated with E-cadherin expression *in vitro* and *in vivo*, particularly in human PDAC specimens in our TMA and RNA sequencing data from The Cancer Genome Atlas.

Finally, as a transcription factor, ESE3 protein has a highly conserved DNA-binding domain and binds to conserved EBSs (GGAA/T) to regulate the promoter/enhancer regions of downstream target genes. Authors reported that as a tumor suppressor, ESE3 binds directly to the promoters of oncogenes (DCDC2, TWIST1, ZEB2, BMI1, and POU5F1) (13,16) and negatively regulates the expression of those genes in prostate tumors. Similarly, ESE3 increases the expression of the tumor suppressor gene caspase-3 (15) at the transcriptional level by binding directly to the caspase-3 promoter. To determine whether ESE3 regulates transcription of E-cadherin in pancreatic cancer cells, we examined the promoter region of the human E-cadherin gene and identified six EBSs. Chromatin immunoprecipitation and luciferase assay results indicated that ESE3 bound directly to the E-cadherin promoter and positively influenced E-cadherin gene expression in PDAC cells.

In summary, we demonstrated that ESE3 expression decreased in PDACs, particularly those with poor differentiation, indicating the relationship of ESE3 expression with poor prognosis for this tumor. ESE3 suppressed PDAC cell metastasis and aggressive PDAC phenotypes *in vitro* and *in vivo*. ESE3 upregulated E-cadherin expression in PDAC cells by binding directly to the EBSs of the E-cadherin gene promoter. Conceivably, the use Decitabine to reduce the methylation of ESE3 promoter could lead to and sustain the expression of ESE3 and reduce cell viability and cell ability to migrate and invade. Therefore, it is possible that the combined use of Decitabine with Gemcitabine may represent a more effective treatment regimen for metastatic PDAC patients.

Supplementary Material

Refer to Web version on PubMed Central for supplementary material.

Acknowledgments

Financial Support

This work was supported by National Science Foundation of China (grants 81502067, 31470951, 81302082, 81272685, 31301151, 81172355, 31471340, 31470957, 81472264, and 81401957), the Major Anticancer Technologies R&D Program of Tianjin (grant 12ZCDZSY16700), and the National Cancer Institute, National Institutes of Health (grants R01CA172233, 1R01CA195651, and R01CA198090).

We thank Don Norwood for editorial assistance.

References

1. Siegel RL, Miller KD, Jemal A. Cancer statistics, 2015. CA: a Cancer journal for clinicians. 2015; 65:5–29. [PubMed: 25559415]

2. Ko AH. Progress in the treatment of metastatic pancreatic cancer and the search for next opportunities. J Clin Oncol. 2015; 33:1779–1786. [PubMed: 25918299]
3. Zhao T, Ren H, Li J, Chen J, Zhang H, Xin W, et al. LASP1 is a HIF1alpha target gene critical for metastasis of pancreatic cancer. Cancer Res. 2015; 75:111–119. [PubMed: 25385028]
4. Ryan DP, Hong TS, Bardeesy N. Pancreatic adenocarcinoma. The New England journal of medicine. 2014; 371:1039–1049. [PubMed: 25207767]
5. Feldman RJ, Sementchenko VI, Watson DK. The epithelial-specific Ets factors occupy a unique position in defining epithelial proliferation, differentiation and carcinogenesis. Anticancer research. 2003; 23:2125–2131. [PubMed: 12894586]
6. Oikawa T, Yamada T. Molecular biology of the Ets family of transcription factors. Gene. 2003; 303:11–34. [PubMed: 12559563]
7. Seth A, Watson DK. ETS transcription factors and their emerging roles in human cancer. European journal of cancer. 2005; 41(16):2462–2478. [PubMed: 16213704]
8. Sharrocks AD. The ETS-domain transcription factor family. Nature Reviews Molecular Cell Biology. 2001; 2:827–837. [PubMed: 11715049]
9. Albino D, Longoni N, Curti L, Mello-Grand M, Pinton S, Civenni G, et al. ESE3/EHF controls epithelial cell differentiation and its loss leads to prostate tumors with mesenchymal and stem-like features. Cancer research. 2012; 72:2889–2900. [PubMed: 22505649]
10. Wang L, Xing J, Cheng R, Shao Y, Li P, Zhu S, Zhang S. Abnormal Localization and Tumor Suppressor Function of Epithelial Tissue-Specific Transcription Factor ESE3 in Esophageal Squamous Cell Carcinoma. PLoS One. 2015; 10:e0126319. [PubMed: 25950810]
11. Taniue K, Oda T, Hayashi T, Okuno M, Akiyama T. A member of the ETS family, EHF, and the ATPase RUVBL1 inhibit p53-mediated apoptosis. EMBO reports. 2011; 12:682–689. [PubMed: 21617703]
12. Kar A, Gutierrez-Hartmann A. Molecular mechanisms of ETS transcription factor-mediated tumorigenesis. Critical reviews in biochemistry and molecular biology. 2013; 48:522–543. [PubMed: 24066765]
13. Albino D, Longoni N, Curti L, Mello-Grand M, Pinton S, Civenni G, et al. ESE3/EHF controls epithelial cell differentiation and its loss leads to prostate tumors with mesenchymal and stem-like features. Cancer research. 2012; 72:2889–2900. [PubMed: 22505649]
14. Albino D, Civenni G, Dallavalle C, Roos M, Jahns H, Curti L, et al. Activation of the Lin28/let-7 Axis by Loss of ESE3/EHF Promotes a Tumorigenic and Stem-like Phenotype in Prostate Cancer. Cancer research. 2016; 76:3629–3643. [PubMed: 27197175]
15. Cangemi R, Mensah A, Albertini V, Jain A, Mello-Grand M, Chiorino G, et al. Reduced expression and tumor suppressor function of the ETS transcription factor ESE-3 in prostate cancer. Oncogene. 2008; 27:2877–2885. [PubMed: 18037958]
16. Longoni N, Kunderfranco P, Pellini S, Albino D, Mello-Grand M, Pinton S, et al. Aberrant expression of the neuronal-specific protein DCDC2 promotes malignant phenotypes and is associated with prostate cancer progression. Oncogene. 2013; 32:2315–2324. 24 e1–24 e4. [PubMed: 22733135]
17. Wang L, Xing J, Cheng R, Shao Y, Li P, Zhu S, et al. Abnormal Localization and Tumor Suppressor Function of Epithelial Tissue-Specific Transcription Factor ESE3 in Esophageal Squamous Cell Carcinoma. PloS one. 2015; 10:e0126319. [PubMed: 25950810]
18. Sotomayor M, Gaudet R, Corey DP. Sorting out a promiscuous superfamily: towards cadherin connectomics. Trends Cell Biol. 2014; 24:524–536. [PubMed: 24794279]
19. van Roy F. Beyond E-cadherin: roles of other cadherin superfamily members in cancer. Nat Rev Cancer. 2014; 14:121–134. [PubMed: 24442140]
20. Hoffman BD, Yap AS. Towards a Dynamic Understanding of Cadherin-Based Mechanobiology. Trends Cell Biol. 2015; 25:803–814. [PubMed: 26519989]
21. Lecuit T, Yap AS. E-cadherin junctions as active mechanical integrators in tissue dynamics. Nat Cell Biol. 2015; 17:533–539. [PubMed: 25925582]
22. Kotiyal S, Bhattacharya S. Events of Molecular Changes in Epithelial-Mesenchymal Transition. Crit Rev Eukaryot Gene Expr. 2016; 26:163–171. [PubMed: 27480779]

23. Hotz B, Arndt M, Dullat S, Bhargava S, Buhr HJ, Hotz HG. Epithelial to mesenchymal transition: expression of the regulators snail, slug, and twist in pancreatic cancer. Clin Cancer Res. 2007; 13:4769–4776. [PubMed: 17699854]
24. Wheelock MJ, Shintani Y, Maeda M, Fukumoto Y, Johnson KR. Cadherin switching. J Cell Sci. 2008; 121:727–735. [PubMed: 18322269]
25. Maeda M, Johnson KR, Wheelock MJ. Cadherin switching: essential for behavioral but not morphological changes during an epithelium-to-mesenchyme transition. J Cell Sci. 2005; 118:873–887. [PubMed: 15713751]
26. Qian X, Anzovino A, Kim S, Suyama K, Yao J, Hulit J, et al. N-cadherin/FGFR promotes metastasis through epithelial-to-mesenchymal transition and stem/progenitor cell-like properties. Oncogene. 2014; 33:3411–3421. [PubMed: 23975425]
27. Shintani Y, Hollingsworth MA, Wheelock MJ, Johnson KR. Collagen I promotes metastasis in pancreatic cancer by activating c-Jun NH(2)-terminal kinase 1 and up-regulating N-cadherin expression. Cancer Res. 2006; 66:11745–11753. [PubMed: 17178870]
28. Su Y, Li J, Witkiewicz AK, Brennan D, Neill T, Talarico J, et al. N-cadherin haploinsufficiency increases survival in a mouse model of pancreatic cancer. Oncogene. 2012; 31:4484–4489. [PubMed: 22158044]
29. Al-Aynati MM, Radulovich N, Riddell RH, Tsao MS. Epithelial-cadherin and beta-catenin expression changes in pancreatic intraepithelial neoplasia. Clin Cancer Res. 2004; 10:1235–1240. [PubMed: 14977820]
30. Pasca di Magliano M, Biankin AV, Heiser PW, Cano DA, Gutierrez PJ, Deramaudt T, et al. Common activation of canonical Wnt signaling in pancreatic adenocarcinoma. PloS One. 2007; 2:e1155. [PubMed: 17982507]
31. Nakajima S, Doi R, Toyoda E, Tsuji S, Wada M, Koizumi M, et al. N-cadherin expression and epithelial-mesenchymal transition in pancreatic carcinoma. Clin Cancer Res. 2004; 10:4125–4133. [PubMed: 15217949]
32. Su Y, Li J, Shi C, Hruban RH, Radice GL. N-cadherin functions as a growth suppressor in a model of K-ras-induced PanIN. Oncogene. 2016; 35:3335–3341. [PubMed: 26477318]
33. Beuran M, Negoi I, Paun S, Ion AD, Bleotu C, Negoi RI, Hostiuc S. The epithelial to mesenchymal transition in pancreatic cancer: A systematic review. Pancreatology. 2015; 15:217–225. [PubMed: 25794655]
34. Xie D, Xie K. Pancreatic cancer stromal biology and therapy. Genes Dis. 2015; 2(2):133–143. [PubMed: 26114155]
35. Guo K, Cui J, Quan M, Xie D, Jia Z, Wei D, et al. A novel KLF4-MSI2 signaling pathway regulates growth and metastasis of pancreatic cancer. Clin Cancer Res. 2016 Jul.:22. pii: clincanres.1064.2016. [Epub ahead of print].
36. Wei D, Wang L, Yan Y, Jia Z, Gagea M, Li Z, et al. KLF4 Is Essential for Induction of Cellular Identity Change and Acinar-to-Ductal Reprogramming during Early Pancreatic Carcinogenesis. Cancer Cell. 2016; 29(3):324–338. [PubMed: 26977883]
37. Yan Y, Li Z, Kong X, Jia Z, Zuo X, Gagea M, et al. KLF4-Mediated Suppression of CD44 Signaling Negatively Impacts Pancreatic Cancer Stemness and Metastasis. Cancer Res. 2016; 76(8):2419–2431. [PubMed: 26880805]
38. Zhou A, Lin K, Zhang S, Chen Y, Zhang N, Xue J, et al. Nuclear GSK3β promotes tumorigenesis by phosphorylating KDM1A and inducing its deubiquitylation by USP22. Nat Cell Biol. 2016; 18(9):954–966. [PubMed: 27501329]
39. Zhao T, Gao S, Wang X, Liu J, Duan Y, Yuan Z, et al. Hypoxia-inducible factor-1alpha regulates chemotactic migration of pancreatic ductal adenocarcinoma cells through directly transactivating the CX3CR1 gene. PloS One. 2012; 7:e43399. [PubMed: 22952674]
40. Yang S, Huang XY. Ca2+ influx through L-type Ca2+ channels controls the trailing tail contraction in growth factor-induced fibroblast cell migration. The Journal of Biological Chemistry. 2005; 280:27130–27137. [PubMed: 15911622]
41. Sainz B Jr, Alcala S, Garcia E, Sanchez-Ripoll Y, Azevedo MM, Cioffi M, et al. Microenvironmental hCAP-18/LL-37 promotes pancreatic ductal adenocarcinoma by activating its cancer stem cell compartment. Gut. 2015; 64:1921–1935. [PubMed: 25841238]

42. Fujisawa T, Joshi B, Nakajima A, Puri RK. A novel role of interleukin-13 receptor alpha2 in pancreatic cancer invasion and metastasis. Cancer Research. 2009; 69(22):8678–8685. [PubMed: 19887609]

43. Gao J, Aksoy BA, Dogrusoz U, Dresdner G, Gross B, Sumer SO, et al. Integrative analysis of complex cancer genomics and clinical profiles using the cBioPortal. Science Signaling. 2013; 6:pl1. [PubMed: 23550210]

44. Cerami E, Gao J, Dogrusoz U, Gross BE, Sumer SO, Aksoy BA, et al. The cBio cancer genomics portal: an open platform for exploring multidimensional cancer genomics data. Cancer Discovery. 2012; 2:401–404. [PubMed: 22588877]

45. Menke A, Philippi C, Vogelmann R, Seidel B, Lutz MP, Adler G, et al. Down-regulation of E-cadherin gene expression by collagen type I and type III in pancreatic cancer cell lines. Cancer Research. 2001; 61:3508–3517. [PubMed: 11309315]

46. Pignatelli M, Ansari TW, Gunter P, Liu D, Hirano S, Takeichi M, et al. Loss of membranous E-cadherin expression in pancreatic cancer: correlation with lymph node metastasis, high grade, and advanced stage. The Journal of pathology. 1994; 174:243–248. [PubMed: 7884585]

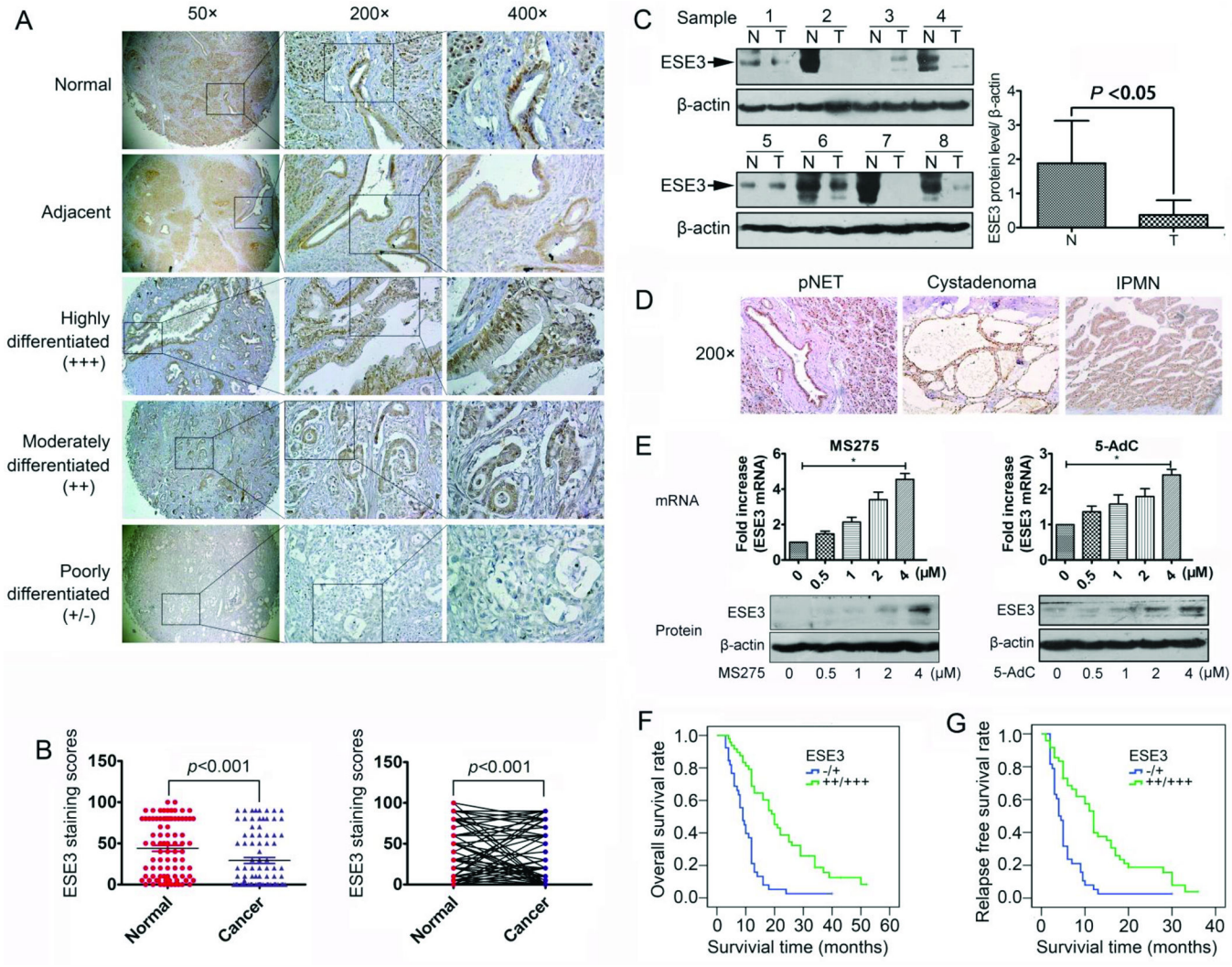

Fig. 1. Reduced ESE3 expression in PDACs predicts poor survival durations

A, immunohistochemical analysis of ESE3 protein expression in TMAs of PDAC and adjacent normal pancreatic tissue specimens. B, analysis of the ESE3 expression in the TMA specimens according to staining scores. C, left panel: Western blotting analysis of ESE3 expression in eight paired human PDAC (T) and matched adjacent normal pancreatic tissue (N) specimens. ESE3 protein expression levels were normalized according to β-actin expression levels. Right panel: ESE3 protein expression levels in PDAC specimens versus paired adjacent normal pancreatic tissue specimens ($n = 8$; $P < 0.05$ [paired t-test]). D, immunohistochemical analysis of ESE3 protein expression in pancreatic neuroendocrine tumor (pNET), serous cystadenoma, and intraductal papillary mucinous neoplasm (IPMN) specimens. E, quantitative reverse transcription-PCR and Western blotting analysis of ESE3 mRNA (upper panel) and protein (lower panel) expression after treatment with MS-275 and 5-AdC for 48 hours. F, association of ESE3 expression with OS rate in patients with PDAC. The patients ($n = 119$) were stratified into two groups according to ESE3 immunohistochemical staining intensity. Patients with low ESE3 expression (intensity grade, −/+) had much shorter OS durations than did patients with high ESE3 expression (intensity

grade, ++/+++; $P < 0.001$ [log-rank test]). G, association of ESE3 expression with RFS rate in PDAC patients ($P < 0.001$ [log-rank test]).

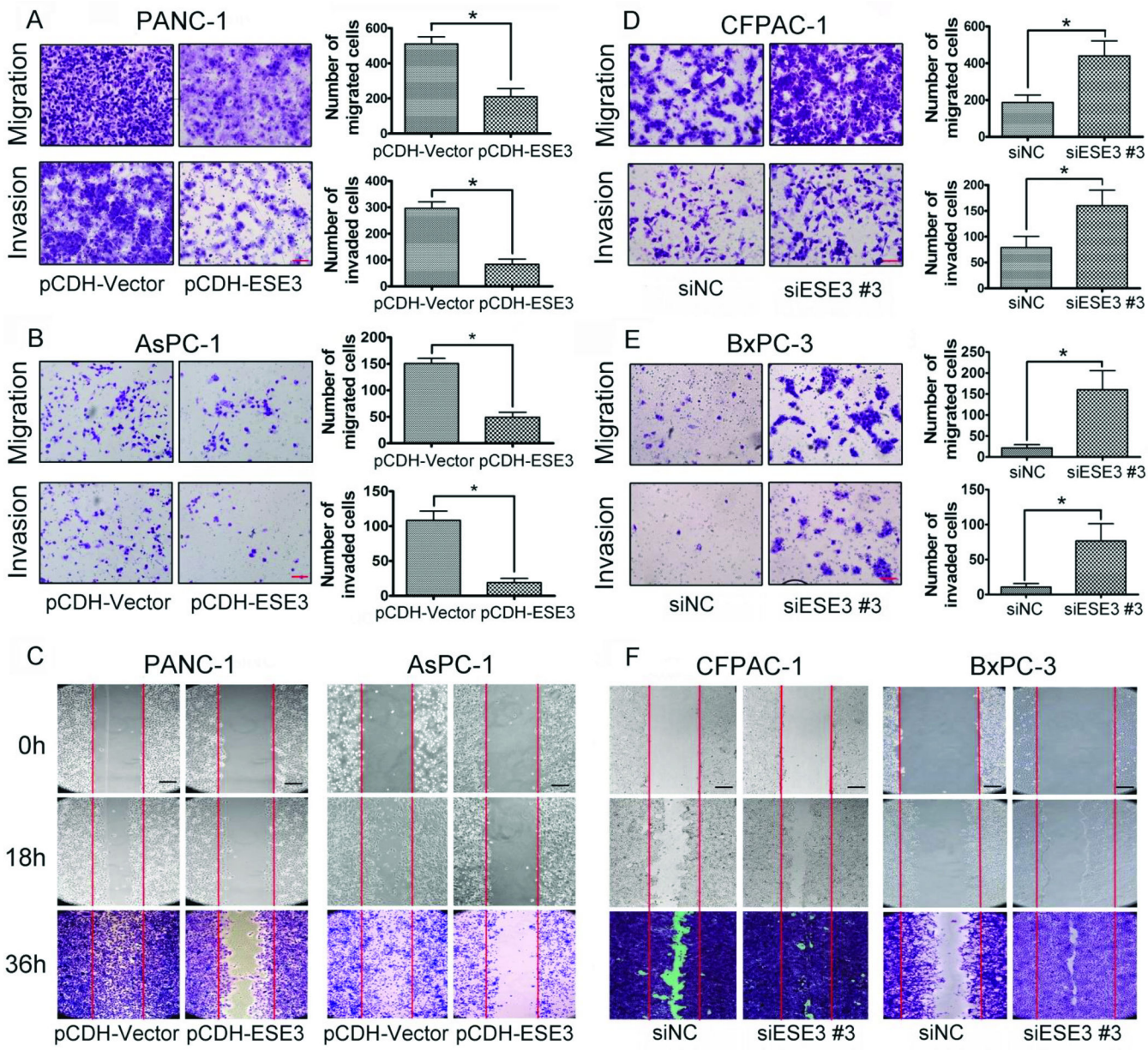

Fig. 2. ESE3 suppresses PDAC cells migration and invasion

A and B, comparison of the migration and invasion of PANC-1 (A) and AsPC-1 (B) cells transfected with pCDH-Vector and pCDH-ESE3 (2 μg) for 48 hours using Boyden chambers. C, wound-healing assays comparing the motility of PANC-1 (left) and AsPC-1 (right) cells transfected with pCDH-Vector or pCDH-ESE3 (2 μg) for 48 hours. D and E, comparison of the migration and invasion of CFPAC-1 (D) and BxPC-3 (E) cells transfected with siNC and siESE3 #3 (50 nM) for 48 hours using Boyden chambers. F, wound-healing assays comparing the motility of CFPAC-1 (left) and BxPC-3 (right) cells transfected with siNC or siESE3 #3 (50 nM) for 48 hours. Magnification, 100×; scale bar = 200 μm. The data are presented as the means ± SEM from three independent experiments. *$P < 0.05$ versus control; scale bar = 100 μm.

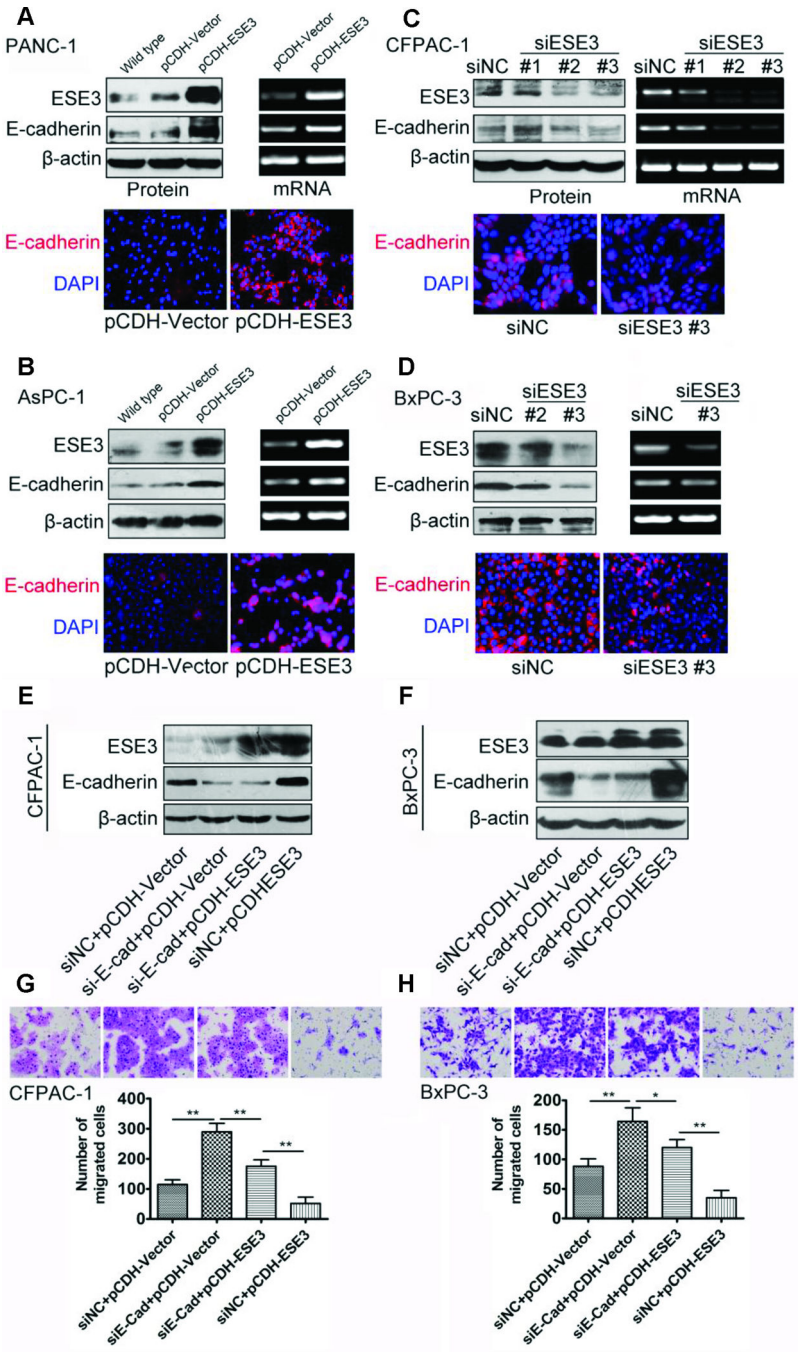

Fig. 3. ESE3 positively regulates E-cadherin expression in PDAC cells

A and B, upper panel: Western blotting and PCR analysis of ESE3 and E-cadherin protein expression in PANC-1 (A) and AsPC-1 (B) cells transfected with pCDH-Vector or pCDH-ESE3 (2 μg) for 48 hours. β-actin was used as a loading control. Lower panel: immunofluorescent images of PANC-1 (A) and AsPC-1 (B) cells transfected with pCDH-Vector or pCDH-ESE3 (2 μg) for 48 hours stained for E-cadherin (red) and DAPI (blue; magnification, 200×). C and D, upper panel: Western blotting and PCR analysis of ESE3 and E-cadherin protein expression in CFPAC-1 (C) and BxPC-3 (D) cells transfected with

negative control siRNA (siNC) or siESE3 #1, #2, or #3 (50 nM) for 48 hours. β-actin was used as a loading control. Lower panel: immunofluorescent images of CFPAC-1 (C) and BxPC-3 (D) cells transfected with siNC or siESE3 #3 (50 nM) for 48 hours stained for E-cadherin (red) and DAPI (blue; magnification, 200×). E and F, Western blotting analysis of CFPAC-1 and BxCP-3 cells co-transfected with siESE3 #3 (50 nmol/L) or pCDH-ESE3 (2 μg). G and H, Boyden chamber analysis of CFPAC-1 and BxCP-3 cells co-transfected with siESE3 #3 (50 nmol/L) or pCDH-ESE3 (2 μg). The data are presented as the means ± SEM from three independent experiments. *$P < 0.05$; **$P < 0.01$. Magnification, 200×.

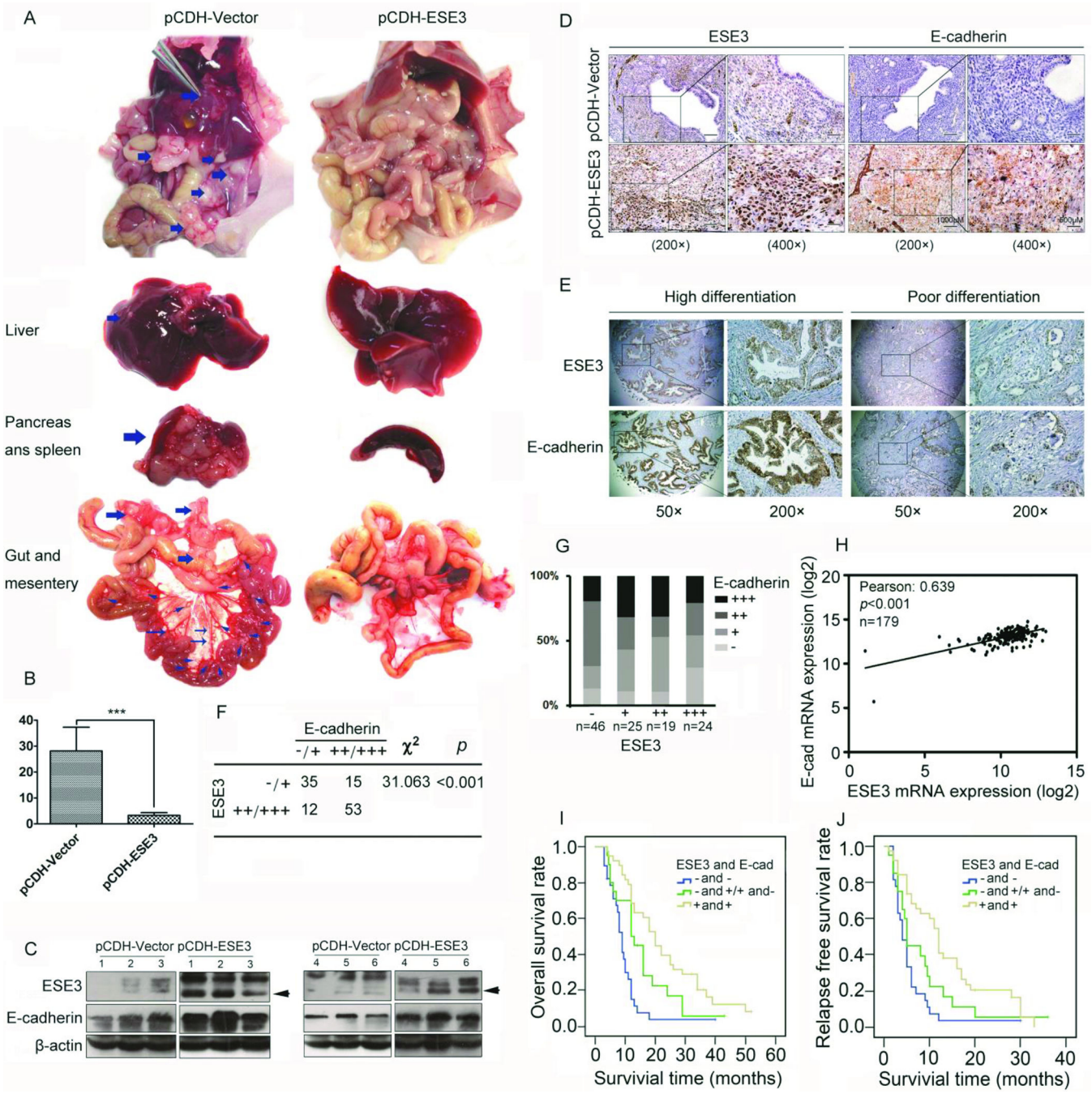

Fig. 4. ESE3 suppresses the metastasis of PDAC in a mouse model, and its expression is positively correlated with E-cadherin expression in human PDAC specimens

A, a mouse model of pancreatic cancer was established via intrasplenic injection of PANC-1/pCDH-Vector or stable PANC-1/pCDH-ESE3 cells in nude mice (n = 5/group). Shown are representative images of primary pancreatic tumors and metastatic tumors in the liver, gut, and mesentery obtained from mice. B, statistical analysis of the total number of visible metastatic lesions in the liver, gut, and mesentery in our mouse model of pancreatic cancer (t-test). The data are presented as the means ± SEM from two independent experiments. ***P < 0.001. C, Western blotting analysis of ESE3 and E-cadherin expression

in orthotopic pancreatic tumors in nude mice injected with PANC-1/pCDH-Vector or stable PANC-1/pCDH-ESE3 cells. D, representative immunohistochemical stains of ESE3 and E-cadherin expression in orthotopic pancreatic tumor specimens (magnification, 200× and 400×). E, immunohistochemical stains of human PDAC specimens showing correlative ESE3 and E-cadherin expression. F, statistical analysis of immunohistochemical staining of human PDAC specimens for ESE3 and E-cadherin expression. G, the distribution of immunohistochemical staining scores for ESE3 and E-cadherin expression in human PDAC specimens. H, correlation analysis of ESE3 and E-cadherin expression in 179 PDAC specimens with RNA sequencing data available from The Cancer Genome Atlas. I, association of ESE3 and E-cadherin expression with OS rate in patients with PDAC. The patients ($n = 119$) were stratified into three groups according to ESE3 and E-cadherin immunohistochemical staining intensity ("−" and "−"; "−" and "+" or "+" and "−"; "+" and "+") ($P < 0.001$ [log-rank test]). J, association of ESE3 and E-cadherin expression with RFS rate in PDAC patients ($P < 0.001$ [log-rank test]).

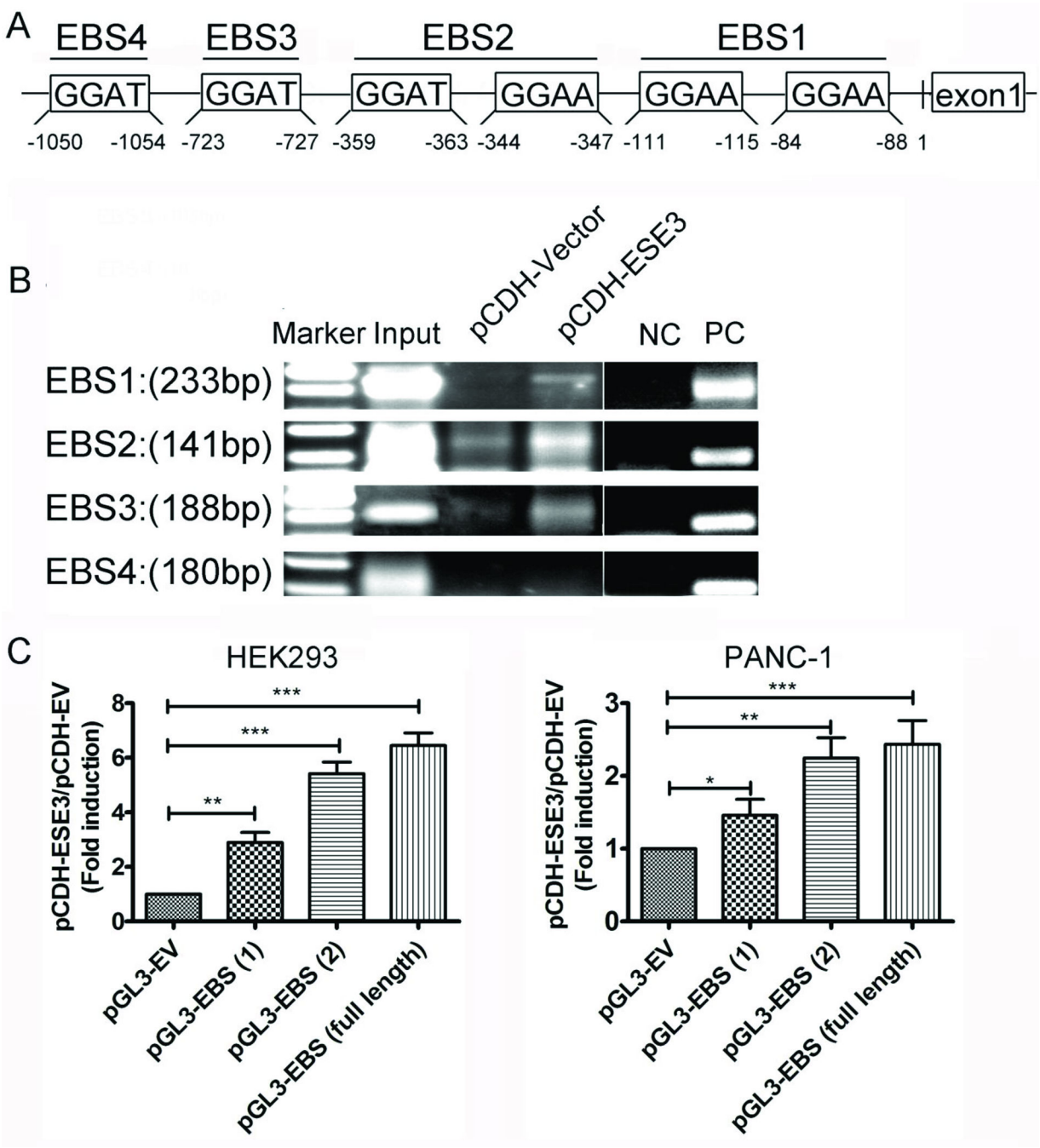

Figure 5. Transcriptional regulation of E-cadherin expression by ESE3 in PDAC cells

A, schematic of the structure of the E-cadherin gene promoter. Shown are six EBSs and their respective locations. B, chromatin immunoprecipitation analysis of ESE3 binding to the E-cadherin promoter in PANC-1/pCDH-Vector and stable PANC-1/pCDH-ESE3 cells. C, luciferase assay-based promoter activity analysis of HEK293 and PANC-1 cells overexpressing ESE3 (pCDH-ESE3) and control cells transfected with pGL3-ESE3(1), pGL3-ESE3(2), pGL3-ESE3 (full length), or pGL3-empty vector (pGL3-EV). Forty-eight hours after transfection, the cells were subjected to dual luciferase analysis. The results are

expressed as fold induction relative to that in corresponding cells transfected with the control vector after normalization of firefly luciferase activity according to Renilla luciferase activity. The data are expressed as the means ± SEM from three independent experiments. *$P < 0.05$; **$P < 0.01$;***$P < 0.001$.

Table 1

Correlation of ESE3 expression to clinicopathological features in PDAC

Parameters		ESE3 (n) −/+	ESE3 (n) ++/+++	χ^2	*P*	*r*
Age (years)				0.248	0.698	−0.048
	<60	23	34			
	≥60	23	28			
Gender				0.212	0.696	0.044
	Male	28	35			
	Female	18	27			
Histological grade				7.275	0.011[a]	−0.260
	G1, G2	29	53			
	G3	17	9			
Tumor size				2.963	0.114	−0.158
	T1	24	42			
	T2	22	20			
LN metastasis				6.358	0.018[a]	−0.243
	N0	20	42			
	N1	26	20			
Vessel invasion				8.058	0.006[a]	−0.273
	M0	21	45			
	M1	25	17			

NOTE: Statistical data on ESE3 expression in relation to clinicohistopathologic features for surgical PDAC specimens. P values were calculated using the chi-square test.

Abbreviation: LN, lymph node.

[a]Statistically significant (P< 0.05).

Table 2

Univariate and multivariate analysis of clinicopathological factors for overall survival (OS) and relapse-free survival (RFS)

Univariate analysis				
Variables	**OS**		**RFS**	
	HR (95.0% CI)	***P***	**HR (95.0% CI)**	***P***
Age	1.279 (0.810–2.019)	0.291	1.265 (0.800–2.001)	0.315
Gender	1.073 (0.681–1.693)	0.761	1.068 (0.675–1.690)	0.780
Tumor size	1.870 (1.181–2.962)	0.008[a]	1.875 (1.176–2.989)	0.008[a]
Vessel invasion	2.870 (1.791–4.600)	0.000[a]	3.134 (1.912–5.137)	0.000[a]
LN metastasis	2.415 (1.520–3.838)	0.000[a]	2.129 (1.336–3.391)	0.001[a]
Grade	2.378 (1.430–3.954)	0.001[a]	3.310 (1.930–5.676)	0.000[a]
ESE3	0.320 (0.196–0.523)	0.000[a]	0.363 (0.223–0.590)	0.000[a]
Multivariate analysis				
Tumor size	1.097 (0.635–1.895)	0.740	1.091 (0.631–1.888)	0.754
Vessel invasion	1.952 (1.159–3.289)	0.012[a]	1.988 (1.141–3.465)	0.015[a]
LN metastasis	1.605 (0.944–2.728)	0.081[a]	1.384 (0.807–2.373)	0.237
Grade	1.749 (1.040–2.942)	0.035	2.041 (1.161–3.587)	0.013[a]
ESE3	0.457 (0.274–0.763)	0.003[a]	0.551 (0.329–0.924)	0.024[a]

NOTE: Univariate analysis: log rank; multivariate Cox proportional hazards analysis.

Abbreviations: HR, hazard ratio; CI, confidence interval; LN, lymph node.

[a]Statistically significant (P< 0.05).